

Architecture Dependence on the Steric Constrains of the Ligand in Cyano-Bridged Copper(II) and Copper(I)–Copper(I) Mixed-Valence Polymer Compounds Containing Diamines: Crystal Structures and Spectroscopic and Magnetic Properties

Enrique Colacio,^{*,#} Raikko Kivekäs,^{*,†} Francesc Lloret,[‡] Markku Sunberg,[†] José Suarez-Varela,[#] Manuel Bardaji,[§] and Antonio Laguna[§]

Departamento de Química Inorgánica, Facultad de Ciencias, Universidad de Granada, 18071 Granada, Spain, Department of Chemistry, Laboratory of Inorganic Chemistry, P.O. Box 55, FIN-00014, University of Helsinki, Helsinki, Finland, Departament de Química Inorgánica/Instituto de Ciencia Molecular, Facultat de Química de la Universitat de Valencia, Dr. Moliner 50, 46100-Burjassot, Valencia, Spain, and Departamento de Química Inorgánica, Instituto de Ciencias de Materiales de Aragón, Universidad de Zaragoza-C.S.I.C., E-50009 Zaragoza, Spain

Received May 22, 2002

A family of cyano-bridged copper(II)–copper(I) mixed-valence polymers containing diamine ligands of formula $[\text{Cu}(\text{pn})_2][\text{Cu}_2(\text{CN})_4]$ (**1**, pn = 1,2-propanediamine), $[\text{Cu}_2(\text{CN})_3(\text{dmen})]$ (**2**, dmen = *N,N*-dimethylethylenediamine), and $[\text{Cu}_3(\text{CN})_4(\text{tmen})]$ (**3**, tmen = *N,N,N',N'*-tetramethylethylenediamine) have been prepared with the aim of analyzing how their architecture may be affected by steric constraints imposed by the diamine ligands. In the absence of diamine and with use of the voluminous NEt_4^+ cation, the copper(I) polymer $[\text{NEt}_4][\text{Cu}_2(\text{CN})_3]$ (**4**) forms. The structure of **1** consists of a three-dimensional diamond-related anionic framework host, $[\text{Cu}_2(\text{CN})_4]^{2-}$, and enclathrated $[\text{Cu}(\text{pn})_2]^{2+}$ cations. The structure of **2** is made of neutral corrugated sheets constructed from fused 18-member nonplanar rings, which contain three equivalent copper(I) and three equivalent copper(II) centers bridged by cyanide groups in an alternative form. The 3D structure of **3** consists of interconnected stair-like double chains built from fused 18-member rings, which adopt a chairlike conformation. Each ring is constructed from two distorted trigonal planar Cu(I) centers, two bent seemingly two-coordinated Cu(I) centers, and two pentacoordinated Cu(II) atoms. The structure **4** is made of planar anionic layers $[\text{Cu}_2(\text{CN})_3]_n^{n-}$ lying on mirror planes and NEt_4^+ cations intercalated between the anionic layers. From the X-ray structural results and calculations based upon DFT theory some conclusions are drawn on the structure–steric factors correlation in these compounds. Compound **1** exhibits very weak luminescence at 77 K with a maximum in the emission spectrum at 520 nm, whereas compound **4** shows an intense luminescence at room temperature with a maximum in the emission spectrum at 371 nm. Polymers **2** and **3** exhibit weak antiferromagnetic magnetic exchange interactions with $J = -0.065(3)$ and $-2.739(5) \text{ cm}^{-1}$, respectively. This behavior have been justified on the basis of the sum of two contributions: one arising from the pure ground-state configuration and the other one from the charge-transfer configuration $\text{Cu}^{\text{I}}-\text{CN}-\text{Cu}^{\text{II}}-\text{CN}-\text{Cu}^{\text{I}}$ that mixes with the ground-state configuration.

Introduction

In recent years, much research interest has been focused on crystal engineering of metal coordination polymers.¹ The

* Address correspondence to these authors. E-mail: ecolacio@ugr.es (E.C.); kivekas@cc.helsinki.fi (R.K.).

Universidad de Granada.

† University of Helsinki.

‡ Universitat de Valencia.

§ Universidad de Zaragoza-C.S.I.C.

rational design of these polymeric structures has important implications for the development of new functional materials with potential applications, among other areas, in zeolite-like materials, molecular selection, ion exchange, electrical conductivity, catalysis, and novel magnetic materials.² A widely used tool for the design and synthesis of coordination frameworks is to assemble inorganic and organic molecules into well-defined supramolecules that may exhibit intriguing

architectures and new topologies. When a linear bidentate bridging molecule is used, the dimensionality of the assembled polymeric structure depends on the geometry of the metal ion. In principle, the control and prediction of crystal structures might be possible when the metal ions have a great tendency to adopt a definite coordination geometry. Thus, octahedral metal ions are expected to afford octahedral networks, whereas tetrahedral metal ions are predisposed to generate diamond-like structures. Prussian-blue and its analogues, which are currently playing a major role in the field of molecular-based magnets,³ are typical examples of octahedral coordination polymers built from octahedral metal ion nodes and bifunctional cyanide ligands as spacer. Tetrahedral nodes, such as Zn^{II} and Cd^{II}, and cyanide ligands, however, generate diamond-like coordination polymers, Zn(CN)₂ and Cd(CN)₂, with 2-fold interpenetration.⁴ These microporous materials can be induced to form a single diamond-like framework by providing in the crystallizing medium suitable template molecules of the correct shape and size to fit snugly into the appropriate cavities. This has been shown to occur for the inclusion compounds of general formula M(CN)₂·G (G is a guest molecule and M = Cd^{II} and Zn^{II})⁵ and in the cationic guest compound [NMe₄][CuZn(CN)₄],⁴ in which half of the total cavities were vacant. Note that this latter compound and the isomorphous host [NMe₄]-[CuCd(CN)₄]⁶ are able to additionally accommodate neutral CCl₄ molecules in the remaining cavities. The incorporation

of ligands LL (where LL is a chelating diamine ligand) into hybrid materials as templating, space filling, and passivating agents may provide new and interesting systems. Thus, it has been reported that from copper(II), cyanide, and ethylenediamine, a single diamond-like mixed-valence compound forms, [Cu(en)₂(H₂O)][Cu₂(CN)₄],⁷ in which half of the cavities are occupied by [Cu(en)₂(H₂O)]²⁺ cations acting as both template and guest. From the prospective of assessing the effect of bulkier diaminealkane ligands on the solid architectures of the Cu(II)/Cu(I) polymer systems, the compounds [Cu(pn)₂][Cu₂(CN)₄] (**1**, pn = 1,2-propanediamine), [Cu₂(CN)₃(dmen)] (**2**, dmen = *N,N*-dimethylethylenediamine), [Cu₃(CN)₄(tmen)] (**3**, tmen = *N,N,N',N'*-tetramethylethylenediamine), and [NEt₄][Cu₂(CN)₃] (**4**) have been prepared and structurally characterized. In addition, herein, we report the electronic and luminescence properties of all these complexes and the magnetic study of the cyanide-bridged mixed-valence complexes **2** and **3**.

Experimental Section

All reagents were obtained from Aldrich and used without further purification. Cyanide salts are toxic and should be handled with *Caution*.

General Method of Preparation. To prepare compounds **1–3** the following standard procedure was used. KCN (1.066 g, 16.4 mmol) was added to a solution prepared by dissolving Cu(NO₃)₂·3H₂O (1.0 g, 4.1 mmol) and the corresponding diamine (12.3 mmol) in 50 mL of water. The resulting colorless solution was slowly layered with a blue solution containing Cu(NO₃)₂·3H₂O (0.5 g, 2.05 mmol) and diamine (6.15 mmol). After several days suitable crystals for X-ray diffraction were growing from the resulting blue solution, which were filtered-off, washed with ethanol and air-dried.

[Cu(pn)₂][Cu₂(CN)₄] (**1**): Brown-blue crystals. Yield 70%. Anal. Calcd for C₁₀H₂₀N₈Cu₃: C, 27.09; H, 4.52; N, 25.28. Found: C, 27.45; H, 4.30; N, 26.10. IR (KBr, cm⁻¹): ν(NH) 3290, 3252; ν(CN) 2081.

[Cu₂(CN)₃(dmen)] (**2**): Green crystals. Yield 65%. Anal. Calcd for C₇H₁₂N₅Cu₂: C, 28.64; H, 4.09; N, 23.87. Found: C, 28.50; H, 3.85; N, 24.10. IR (KBr, cm⁻¹): ν(NH) 3335, 3284; ν(CN) 2143, 2125, 2089.

[Cu₃(CN)₄(tmen)] (**3**): Green crystals. Yield 60%. Anal. Calcd for C₁₀H₁₆N₆Cu₃: C, 29.22; H, 3.90; N, 20.46. Found: C, 29.10; H, 4.05; N, 20.70. IR (KBr, cm⁻¹): ν(CN) 2145, 2125.

[NEt₄][Cu₂(CN)₃] (**4**): A solution of Cu(NO₃)₂·3H₂O (1.0 g, 4.1 mmol) in 50 mL of NH₄OH (6M) was reduced with KCN (1.066 g, 16.4 mmol) and the mixture was stirred until a clear colorless solution was obtained. Solid Cu(NO₃)₂·3H₂O (0.5 g, 2.05 mmol) and Et₄NPF₆ were then added with stirring and the essentially clear solution was filtered to eliminate any amount of insoluble material. From the resulting solution at room temperature colorless crystals began to appear after 2 days. Yield 65%. Anal. Calcd for C₁₁H₂₀N₄Cu₂: C, 39.36; H, 5.96; N, 16.70. Found: C, 39.50; H, 5.67; N, 17.10. IR (KBr, cm⁻¹): ν(CN) 2118.

Physical Measurements. Elemental analyses were carried out at the Instrumentation Scientific Center of the University of Granada on a Fisons-Carlo Erba analyzer model EA 1108. IR spectra were recorded on a MIDAC progress-IR spectrometer with KBr pellets.

- (1) Robson, R.; Abraham, B. F.; Batten, S. R.; Gable, R. W.; Hoskins, B. F.; Liu, J. In *Supramolecular Architecture*; Bein, T., Ed.; American Chemical Society: Washington, DC, 1992; Chapter 19, p 258. Robson, R. In *Comprehensive Supramolecular Chemistry*; Pergamon: New York, 1996; Chapter 22, p 733. *Crystals Engineering: The Design and Applications of Functional Solids*; Seddon, K. R., Zaworotko, M. J., Eds.; NATO Science Series C; Kluwer Academic Publishers: Dordrecht, The Netherlands, 1999; Vol. 539. Zaworotko, M. J. *Angew. Chem., Int. Ed.* **2000**, *39*, 3052. Kitagawa, S.; Kondo, M. *Bull. Chem. Soc. Jpn.* **1998**, *71*, 1739. Blake, A. J.; Champness, N. R.; Hubberstey, P.; Li, W. S.; Withersby, M. A.; Schröder, M. *Coord. Chem. Rev.* **1999**, *183*, 117.
- (2) Yaghi, O. M.; Li, G.; Li, H. *Nature* **1995**, *378*, 703. Yaghi, O. M.; Li, H.; Groy, T. L. *J. Am. Chem. Soc.* **1996**, *118*, 9096. Yaghi, O. M.; Li, H. *J. Am. Chem. Soc.* **1995**, *117*, 10401. Yaghi, O. M.; Li, H. *J. Am. Chem. Soc.* **1996**, *118*, 295. Li, H.; Eddaoudi, M.; O'Keefe, M.; Yaghi, O. M. *Nature* **1999**, *402*, 276. Kondo, M.; Okubo, T.; Asami, A.; Noro, S.; Yoshimoto, T.; Kitagawa, S.; Ishii, T.; Matsuzaka, H.; Seki, K. *Angew. Chem., Int. Ed.* **1999**, *38*, 140. Fujita, M.; Kwon, Y. J.; Washizu, S.; Ogura, K. *J. Am. Chem. Soc.* **1994**, *116*, 1151. Kondo, M.; Yoshimoti, T.; Seki, K.; Matsuzaka, H.; Kitagawa, S. *Angew. Chem., Int. Ed.* **1997**, *36*, 1725. Noro, S.; Kitagawa, S.; Kondo, M.; Seki, K. *Angew. Chem., Int. Ed.* **2000**, *39*, 2082. *Magnetism: A Supramolecular Function*; Kahn, O., Eds.; NATO ASI Series C484; Kluwer Academic Publishers: Dordrecht, The Netherlands, 1996. *Molecular Magnetism: From the Molecular Assemblies to the Devices*; Coronado, E., Delhaés, P., Gatteschi, D., Miller, J. S., Eds.; NATO ASI Series E321; Kluwer Academic Publishers: Dordrecht, The Netherlands, 1996; pp 43, 179. Coronado, E.; Galán-Mascarós, J. R.; Gómez-García, C. J.; Laukhin, V. *Nature* **2000**, *408*, 447.
- (3) Dumber, K. R.; Heintz, R. A. *Prog. Inorg. Chem.* **1997**, *45*, 283. Verdager, M. *Science* **1996**, *272*, 698. Entley, W.; Girolami, G. S. *Science* **1995**, *268*, 397. Ferlay, S.; Mallah, T.; Ouahes, R.; Veillet, P.; Verdager, M. *Nature* **1995**, *378*, 701. Verdager, M.; Bleuzen, A.; Marvaud, V.; Vaissermann, J.; Seuleiman, M.; Desplanches, C.; Sculler, A.; Train, C.; Garde, R.; Gelly, G.; Lomenech, C.; Rosenman, I.; Veillet, P.; Cartier, C.; Villain, F. *Coord. Chem. Rev.* **1999**, *190*, 1023. Ohba, M.; Okawa, K. *Coord. Chem. Rev.* **2000**, *198*, 313. Rogez, G.; Parsons, M. S.; Villar, V.; Mallah, T. *Inorg. Chem.* **2001**, *40*, 3836.
- (4) Hoskins, B. F.; Robson, R. *J. Am. Chem. Soc.* **1990**, *112*, 1546.
- (5) Abrahams, B. F.; Hoskins, B. F.; Liu, J. P.; Robson, R. *J. Am. Chem. Soc.* **1991**, *113*, 3045. Kitazawa, T.; Nishikiori, S.; Yamagishi, A.; Kuroda, R.; Iwamoto, T. *J. Chem. Soc., Dalton Trans.* **1992**, 413.

(6) Kitazawa, T.; Nishikiori, S.; Kuroda, R.; Iwamoto, T. *J. Chem. Soc., Dalton Trans.* **1994**, 1029.

(7) Williams, R. J.; Larson, A. C.; Cromer, D. T. *Acta Crystallogr. Sect. B* **1972**, *28*, 858.

Table 1. Crystallographic Data and Structural Refinement Details for Compounds **1**, **2**, **3**, and **4**

	1	2	3	4
empirical formula	C ₁₀ H ₂₀ Cu ₃ N ₈	C ₇ H ₁₂ Cu ₂ N ₅	C ₁₀ H ₁₆ Cu ₃ N ₆	C ₁₁ H ₂₀ Cu ₂ N ₄
fw	442.96	293.30	410.91	335.39
cryst syst	monoclinic	orthorhombic	orthorhombic	orthorhombic
space group	<i>P2₁/n</i> (No. 14)	<i>Pna2₁</i> (No. 33)	<i>Pnma</i> (No. 62)	<i>Ibam</i> (No. 72)
<i>a</i> (Å)	13.506(3)1	13.665(3)	13.787(3)	14.857(4)
<i>b</i> (Å)	8.444(2)	9.989(2)	9.175(2)	8.133(3)
<i>c</i> (Å)	13.580(3)	8.389(2)	12.018(2)	12.240(5)
β (deg)	103.83(3)	90	90	90
<i>V</i> (Å ³)	1503.8(6)	1145.1(4)	1520.2(5)	1479.0(9)
<i>Z</i>	4	4	4	4
<i>T</i> (°C)	−80	−80	−80	−80
λ (Å)	0.71069	0.71069	0.71069	0.71069
ρ (g cm ^{−3})	1.956	1.701	1.795	1.506
μ (cm ^{−1})	42.09	36.84	41.53	28.61
goodness-of-fit	1.024	1.027	1.010	1.045
R1 ^a [<i>I</i> > 2 σ (<i>I</i>)]	0.0652	0.0439	0.0520	0.514
wR2 ^b [<i>I</i> > 2 σ (<i>I</i>)]	0.1269	0.1024	0.1370	0.1341
Flack parameter <i>x</i>		−0.02(6)		

$$^a R1 = \sum ||F_o| - |F_c|| / \sum |F_o|. \quad ^b wR2 = \{ \sum [w(F_o^2 - F_c^2)^2] / \sum [w(F_o^2)^2] \}^{1/2}.$$

Magnetization and variable-temperature (1.7–300 K) magnetic susceptibility measurements on polycrystalline samples of **2** and **3** were carried out with a Quantum Design SQUID operating at different magnetic fields. Experimental susceptibilities were corrected for diamagnetism (-150×10^{-6} and -210×10^{-6} cm³ mol^{−1} for **2** and **3**, respectively), temperature-independent paramagnetism ($+60 \times 10^{-6}$ cm³ mol^{−1} per Cu(II) ion), and the magnetization of the sample holder. The luminescence spectra were recorded on a Perkin-Elmer LS-50B spectrofluorometer by using a dispersion of the samples into KBr.

Crystallography. Single-crystal data collections were performed at -80 °C on a Rigaku AFC7S diffractometer, using graphite monochromatized Mo K α radiation. A total of 2717, 1108, 1646, and 709 unique reflections were collected by $\omega/2\theta$ scan mode ($2\theta_{\max} = 50.5^\circ$) for **1**, **2**, **3**, and **4**, respectively.

The structures were solved by direct methods and refined on F^2 by the SHELXL97 program.⁸ For **1**, **3**, and **4**, refinement of each CN bridge between two Cu(I) atoms indicated disordering with respect to the C and N termini. However, as refinements of site occupation parameters of the bridging CN atom positions did not reduce markedly the *R* values but only made convergence more difficult, fixed occupancies of 50% C and 50% N were adopted for each disordered CN atom position. For each structure, the disordered CN atom positions were labeled in tables and drawings with $\times 1$, $\times 2$, $\times 3$, etc. For all structures, the hydrogen atoms were treated as riding atoms, using the SHELX97 default parameters.

For **1**, in addition to the [Cu₂CN₄]^{2−} fragment, the asymmetric unit of the structure contains also two halves of two partially disordered centrosymmetric [Cu(pn)₂]²⁺ cations. In each cation, the central metal atom occupies the center of inversion, the nitrogen atoms and the methyl carbon occupy one position, but the remaining two carbon atoms are disordered and occupy two positions. Refinement of the structure in the lower symmetry space group *Pc* also indicated disordering of the pn ligands.

For **2**, carbon atoms of the dmen ligand were refined with isotropic displacement parameters but rest of the non-hydrogen atoms with anisotropic displacement parameters. **2** crystallizes in a noncentrosymmetric space group, and absolute configuration of **2** was determined by refinement of the Flack *x* parameter.

For **3**, the tmen ligand is disordered with the N4 atom occupying one position at a mirror plane but the rest of the atoms occupying

Table 2. Selected Bond Lengths (Å) and Angles (deg) for **1**

Cu1–X1	2.089(8)	Cu2–X8 ^b	2.036(8)
Cu1–X3	1.962(10)	Cu2–X4 ^c	2.099(8)
Cu1–X5	1.992(10)	Cu3–N5	1.981(8)
Cu1–X6 ^a	2.016(8)	Cu3–N6	1.984(8)
Cu2–X2	1.938(10)	Cu4–N8	2.004(7)
Cu2–X7	1.981(10)	Cu4–N9	1.979(7)
X1–Cu1–X3	109.1(3)	X2–Cu2–X8 ^b	105.2(3)
X1–Cu1–X5	108.0(3)	X7–Cu2–X8 ^b	109.6(3)
X1–Cu1–X6 ^a	101.2(3)	X2–Cu2–X4 ^c	111.2(3)
X3–Cu1–X5	119.6(4)	X7–Cu2–X4 ^c	98.0(3)
X3–Cu1–X6 ^a	106.0(3)	X8 ^b –Cu2–X4 ^c	101.2(3)
X5–Cu1–X6 ^a	111.3(3)	N5–Cu3–N6	84.9(3)
X2–Cu2–X7	128.6(3)	N8–Cu4–N9	85.8(3)

^{a–c} Equivalent positions: (a) $-x + 5/2, y - 1/2, -z + 3/2$; (b) $-x + 3/2, y + 1/2, -z + 3/2$; (c) $x - 1/2, -y + 1/2, z - 1/2$.

Table 3. Selected Bond Lengths (Å) and Angles (deg) for **2**

Cu1–N1	1.996(8)	Cu1–N5	2.024(8)
Cu1–N2	1.987(9)	Cu2–C1	1.918(8)
Cu1–N3	2.161(10)	Cu2–C3 ^a	1.922(12)
Cu1–N4	2.063(7)	Cu2–C2 ^b	1.947(10)
N1–Cu1–N2	88.9(4)	N4–Cu1–N5	84.6(3)
N1–Cu1–N3	93.8(4)	C1–Cu2–C3 ^a	122.4(6)
N1–Cu1–N4	169.2(4)	C1–Cu2–C2 ^b	121.7(5)
N2–Cu1–N3	104.5(4)	C3 ^a –Cu2–C2 ^b	115.8(5)
N2–Cu1–N5	156.0(4)		

^{a,b} Equivalent positions: (a) $-x + 1/2, y - 1/2, z - 1/2$; (b) $-x + 1/2, y - 1/2, z + 1/2$.

two positions on both sides of the mirror plane. Disordered non-hydrogen atoms of tmen were refined with isotropic displacement parameters but rest of the non-hydrogen atoms with anisotropic displacement parameters. The ligand tmen is disordered also in lower symmetry space group *Pna2₁*.

For **4**, all non-hydrogen atoms were refined with anisotropic displacement parameters.

Crystal data and details of the data collection and refinement for the compounds are summarized in Table 1. Bond lengths and angles for compound **1–4** are gathered in Tables 2–5, respectively.

Computational Details. The structures of four copper(II) complex cations [Cu(en)₂(H₂O)]²⁺, [Cu(pn)₂]²⁺, [Cu(dmen)₂]²⁺, and [Cu(tmen)₂]²⁺ were optimized by the methods based upon DFT theory. In the ADF program package,⁹ the results were obtained with Becke-Perdew (BP) exchange-correlation functional.¹⁰ For the Cu atom the triple- ξ STO basis set augmented by polarization (from

(8) Sheldrick, G. M. *SHELX97*; University of Göttingen: Göttingen, Germany, 1997.

Table 4. Selected Interatomic Distances (Å) and Angles (deg) for **3**

Cu1–N1	1.969(6)	Cu2–X1	1.919(6)
Cu1–N2	2.052(4)	Cu2–C2 ^a	2.437(4)
Cu1–N4	2.058(5)	Cu2···Cu3 ^a	2.5023(11)
Cu1–N5a	2.107(6)	Cu3–C2	1.927(5)
Cu2–C1	1.893(6)	Cu3–X2 ^b	1.938(5)
N2 ^c –Cu1–N2	121.4(2)	X1–Cu2–C2 ^a	110.22(16)
N1–Cu1–N4	175.2(2)	C1–Cu2–C2 ^d	102.01(17)
N2–Cu1–N5a ^c	113.2(3)	C2 ^a –Cu2–C2 ^d	90.7(2)
N2–Cu1–N5a	125.4(3)	C2 ^e –Cu3–C2	128.3(3)
C1–Cu2–X1	133.3(3)	C2–Cu3–X2 ^b	115.68(13)
C1–Cu2–C2 ^a	102.01(17)		

^{a–e} Equivalent positions: (a) $-x + 1/2, -y + 1, z + 1/2$; (b) $-x + 1, -y + 1, -z + 2$; (c) $x, -y + 3/2, z$; (d) $-x + 1/2, y + 1/2, z + 1/2$; (e) $x, -y + 1/2, z$.

Table 5. Selected Bond Lengths (Å) and Angles (deg) for **4**

Cu–X3	1.904(6)	Cu–X1	1.943(5)
Cu–X3 ^a	1.917(7)	N3–C3	1.513(4)
X3–Cu–X2 ^a	135.4(2)	X2–X1–Cu	171.3(5)
X3–Cu–X1	113.3(2)	X1–X2–Cu ^b	168.8(5)
X2 ^a –Cu–X1	111.3(2)	X3 ^c –X3–Cu	177.0(7)

^{a–c} Equivalent positions: (a) $-x + 1/2, y + 1/2, -z + 1$; (b) $-x + 1/2, y - 1/2, -z + 1$; (c) $-x, -y, -z + 1$.

ADF database IV) was employed for the Cu atoms, with 1s–2p electrons treated as a frozen core. For the other atoms the triple- ξ STO basis set was applied, but with double polarization. For C and N atoms the 1s electrons were frozen. The relativistic effect was not taken into account. The volumes of the optimized complex units were then computed at the B3LYP/6-311g** level of theory (level III) by making use of the Gaussian 98 program package.¹¹ No symmetry restrictions were applied during the optimization for [Cu(en)₂(H₂O)]²⁺; in the other complexes the copper(II) cation was always sitting at the center of symmetry.

Results and Discussion

It is well-known that in aqueous solution copper(II) is easily reduced to copper(I) by cyanide. However, with good σ -electron donor ligands that have their greater affinity for Cu(II), it is possible to stabilize Cu(II) sites allowing the isolation of mixed-valence Cu(I)/Cu(II) materials.¹² Thus, in the presence of amine ligands the Cu(II) state is favored and then Cu(I) is oxidized to Cu(II). Owing to the high

stability constants of bis(chelate)copper(II) complexes, chelating diamine ligands, such as ethylenediamine, are expected to strongly favor the oxidation process. In fact, when CuCN is dissolved in a solution of 50% ethylenediamine in water and the resulting solution is allowed to stand at room temperature for several days, purple crystals of the mixed-valence compound [Cu(en)₂(H₂O)][Cu₂(CN)₄] form.⁷ It should be noted that a few cyano-bridged Cu(I)/Cu(II) mixed-valence complexes have been reported so far and, to the best of our knowledge, only three of them are stable polymers with cyano-bridged Cu^I–CN–Cu^{II} units, [Cu₄(CN)₆Cu^{II}(NH₃)₂]_n,¹³ [Cu^ICu^{II}(CN)₄(NH₃)₃]_n,¹⁴ and [Cu(dien)(CN)₂Cu^I(CN)]_n (dien = diethylenetriamine).¹² In view of this and with the aim of analyzing how the architecture of the mixed-valence polymer compounds may be affected by steric constraints imposed by bulkier diamine ligands, we have prepared complexes **1–4**. Crystals of the assembled systems **1–3** were obtained by diffusion of two aqueous solutions of the respective precursors, one containing a mixture of soluble cyanocuprate(I) complexes (prepared from the chemical reduction of Cu(II) with an excess of KCN in the presence of the corresponding diamine) and the other one containing the corresponding bis(diamine)copper(II) complex. When the Et₄N⁺ cation is used as template agent instead of the [Cu(N–N)₂]²⁺ cation (N–N = diamine), complex **4** forms. In this case, to avoid the precipitation of CuCN and to ensure the complete reduction of the Cu(II) ion, aqueous ammonia as well as a greater excess of KCN were used. It should be pointed out that, recently, Stocker and co-workers¹⁵ have prepared a series of extended cyano-bridged Cu(I) systems from the reaction of CuCN and straight-chain diamines. Their synthetic method uses a very reductive aqueous solution containing CuCN and S₂O₃²⁻ and elevated temperatures (in the 358–368 K temperature range) and consequently no mixed-valence complexes were obtained.

Structures. The structure of **1** (Figure 1) is very similar to that of [Cu(en)₂(H₂O)][Cu₂(CN)₄]⁷ and consists of a three-dimensional diamond-related anionic framework host, [Cu₂(CN)₄]²⁻, and enclathrated and disordered [Cu(pn)₂]²⁺ cations, which adopt a charge-compensating and space-filling role in the material. Since the anionic matrix [Cu₂(CN)₄]²⁻ generates as many adamantane cavities as there are tetrahedral centers, only half of the total cavities have to be filled with [Cu(pn)₂]²⁺ cations for charge balance. There are two crystallographically nonequivalent copper(I) atoms in the [Cu₂(CN)₄]²⁻ hosting framework, Cu(1) and Cu(2). The presence of two kinds of metal centers generates two kinds of adamantane cavities in equal numbers: one type is surrounded by four Cu(1) and six Cu(2) metals and designed as Cu(1)₄Cu(2)₆, the other cavities are of the Cu(1)₆Cu(2)₄ type. Each adamantane cavity containing a [Cu(pn)₂]²⁺ cation shares a chair-form cyclohexane-like window with each of four neighboring vacant cavities and vice versa.

- (9) (a) ADF Program System, Release 1999.02, Vrije Universiteit, Theoretical Chemistry, Amsterdam, The Netherlands. (b) Baerends, E. J.; Ellis, D. E.; Ros, P. *Chem. Phys.* **1973**, *2*, 41–51. (c) Versluis, L.; Ziegler, T. *J. Chem. Phys.* **1988**, *88*, 322–328. (d) te Velde, G.; Baerends, E. J. *J. Comput. Phys.* **1992**, *99*, 84–98. (e) Fonseca Guerra, C.; Snijders, J. G.; te Velde, G.; Baerends, E. J. *Theor. Chem. Acc.* **1998**, *99*, 391–403.
- (10) (a) Becke, A. D. *Phys. Rev. A* **1988**, *38*, 3098–3100. (b) Perdew, J. P. *Phys. Rev. B* **1986**, *33*, 8822–8824. (c) Perdew, J. P. *Phys. Rev. B* **1986**, *34*, 7406.
- (11) Frisch, M. J.; Trucks, G. W.; Schlegel, H. B.; Scuseria, G. E.; Robb, M. A.; Cheeseman, J. R.; Zakrzewski, V. G.; Montgomery, J. A., Jr.; Stratmann, R. E.; Burant, J. C.; Dapprich, S.; Millam, J. M.; Daniels, A. D.; Kudin, K. N.; Strain, M. C.; Farkas, O.; Tomasi, J.; Barone, V.; Cossi, M.; Cammi, R.; Mennucci, B.; Pomelli, C.; Adamo, C.; Clifford, S.; Ochterski, J.; Petersson, G. A.; Ayala, P. Y.; Cui, Q.; Morokuma, K.; Malick, D. K.; Rabuck, A. D.; Raghavachari, K.; Foresman, J. B.; Cioslowski, J.; Ortiz, J. V.; Stefanov, B. B.; Liu, G.; Liashenko, A.; Piskorz, P.; Komaromi, I.; Gomperts, R.; Martin, R. L.; Fox, D. J.; Keith, T.; Al-Laham, M. A.; Peng, C. Y.; Nanayakkara, A.; Gonzalez, C.; Challacombe, M.; Gill, P. M. W.; Johnson, B. G.; Chen, W.; Wong, M. W.; Andres, J. L.; Head-Gordon, M.; Replogle, E. S.; Pople, J. A. *Gaussian 98*, Gaussian, Inc.: Pittsburgh, PA, 1998.
- (12) Huang, S. F.; Wei, H. H.; Wang, Y. *Polyhedron* **1997**, *16*, 1747.

- (13) Kappestein, C.; Schubert, U. *J. Chem. Soc., Chem. Commun.* **1980**, 1116.
- (14) Williams, R. J.; Cromer, D. T.; Larson, A. C. *Acta Crystallogr.* **1971**, *B27*, 1701.
- (15) Stocker, F. B.; Staeva, T. P.; Rienstra, C. M.; Britton, D. *Inorg. Chem.* **1999**, *38*, 984.

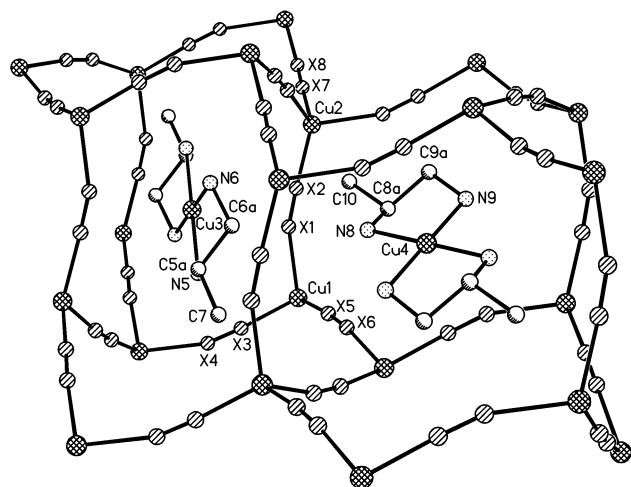


Figure 1. A fragment of the 3D diamond-related anionic framework host $[\text{Cu}_2(\text{CN})_4]^{2-}$ enclathrating $[\text{Cu}(\text{pn})_2]^{2+}$ template cations for **1**. Atoms from the disordered CN bridging groups are labeled as X.

Table 6. The Molar Volumes of the Optimized Complex Cations $[\text{Cu}(\text{N-N})_2]^{2+}$

complex cation	molar vol ($\text{cm}^3 \text{mol}^{-1}$)
$[\text{Cu}(\text{en})_2(\text{H}_2\text{O})]^{2+}$	125.5
$[\text{Cu}(\text{pn})_2]^{2+}$	160.6
$[\text{Cu}(\text{dmen})_2]^{2+}$	169.6
$[\text{Cu}(\text{tmen})_2]^{2+}$	213.6

As for the disordered guest $[\text{Cu}(\text{pn})_2]^{2+}$ cations, the two crystallographically nonequivalent copper(II) centers exhibit symmetrically imposed slightly distorted square-planar CuN_4 coordination environments as the copper(II) ions are located at centers of symmetry. When the structures of $[\text{Cu}(\text{en})_2(\text{H}_2\text{O})][\text{Cu}_2(\text{CN})_4]$ and **1** are compared one realizes that the main factor promoting the decrease in the coordination number of the copper(II) center on going from $[\text{Cu}(\text{en})_2(\text{H}_2\text{O})][\text{Cu}_2(\text{CN})_4]$ to **1** might be the bigger size of the pn ligand with regard to the en ligand. Thus, when the bulkier pn ligand is used, in order to minimize steric interactions the copper(II) ion adopts, instead of the square-pyramidal geometry observed for $[\text{Cu}(\text{en})_2(\text{H}_2\text{O})][\text{Cu}_2(\text{CN})_4]$, a square-planar geometry, which occupies less space and furthermore is electronically favored over the tetrahedral one. The molar volumes for $[\text{Cu}(\text{en})_2(\text{H}_2\text{O})]^{2+}$ and $[\text{Cu}(\text{pn})_2]^{2+}$, calculated from the optimized structures by using DFT methods (see Table 6), support the above hypothesis. With the exception of the intermolecular contact between Cu4 and the adjacent X4 atom of 3.041 Å, the closest contacts involving the guest cations and the hosting $[\text{Cu}_2(\text{CN})_4]^{2-}$ framework (in the range 3.4–3.7 Å) are longer than the sum of the corresponding van der Waals radii, clearly indicating that no significant steric crowding exists in the structure and then the holes are very suitable for the guest $[\text{Cu}(\text{pn})_2]^{2+}$ cations. It should be noted at this point that the $[\text{Cu}(\text{en})_2(\text{H}_2\text{O})]^{2+}$ and $[\text{Cu}(\text{pn})_2]^{2+}$ cations must play a template role in the assembly of the anionic diamond-related framework, since the reaction of Cu(II) with KCN (1:4) in water solution and in the absence of ethylenediamine gives rise to insoluble CuCN together with various cyano complex ions in solution. Complex **1** is a Robin and Day¹⁶ class I mixed-valence compound as the valencies are totally localized.

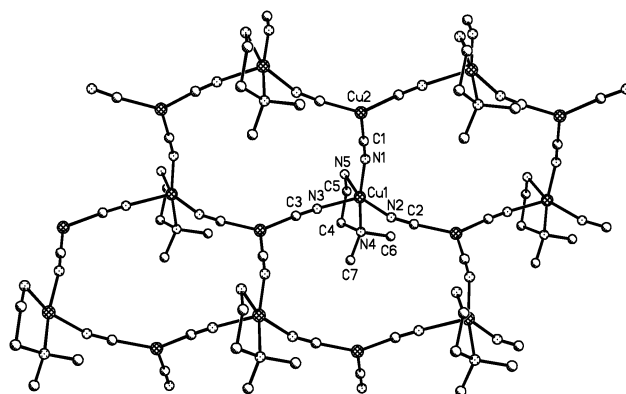


Figure 2. Perspective view of the neutral corrugated sheets of **2**.

The successful isolation of $[\text{Cu}(\text{en})_2(\text{H}_2\text{O})][\text{Cu}_2(\text{CN})_4]$ and **1** demonstrates that diamond-related three-dimensional frameworks can accommodate not only small molecules or cations but also large transition metal cations. This highlights the feasibility of engineering metal–cyanide solids enclathrating transition metal complexes with potentially interesting and useful properties.

The structure of **2** (Figure 2) consists of neutral corrugated sheets constructed from fused 18-member nonplanar rings. Each ring is built from three equivalent copper(I) and three equivalent copper(II) centers, which are bridged by cyanide groups in an alternative form with Cu(I)–Cu(II) distances from 4.9721 (15) to 5.208(2) Å. The bridging fragments Cu(II)–NC–Cu(I) are not linear with both Cu(II)–N–C and Cu(I)–C–N bond angles showing wide variation (160.8(9)–176.7(11)°). Copper(I) centers exhibit a slightly distorted trigonal planar coordination geometry whereas copper(II) centers display a distorted square-pyramidal CuN_5 coordination environment with $\tau = 0.23$ (τ defined as $\alpha - \beta/60$, α and β being the bigger bond angles around copper; $\tau = 0$ for an ideal square pyramid; and $\tau = 1$ for a trigonal bipyramid).¹⁷ In this description, the nitrogen atoms of the diamine ligand occupy basal positions whereas three nitrogen atoms of bridging cyanide groups are situated in the remaining coordination positions. Because the bond angles between the bridging cyanide groups around copper(II) range from 88.8(4) to 104.5(4)° sheets are not planar but very corrugated. The intersheet distance between mean-square planes through the atoms of the sheets is 13.665 Å.

The structure of **3** is made of stair-like double chains running in the direction of the *b*-axis and the double chains are interconnected to afford a 3D network (Figure 3). The double chains are built from fused 18-member rings, which adopt a chairlike conformation. Each ring is constructed from two distorted trigonal-planar Cu(I) centers, two bent seemingly two-coordinated Cu(I) centers, two Cu(II) atoms with a slightly distorted trigonal-bipyramidal CuN_5 coordination polyhedron ($\tau = 0.9$), and six cyanide groups that bridge copper centers, the baricenter of the 18-membered ring lying on an inversion center. The bond angle of the seemingly two-

(16) Robin, M. B.; Day, P. *Adv. Inorg. Chem. Radiochem.* **1967**, *10*, 247.

(17) Addison, A. W.; Rao, T. N.; Reedijk, J.; van Rijn, J.; Verschoor, G. *C. J. Chem. Soc., Dalton Trans.* **1984**, 1349.

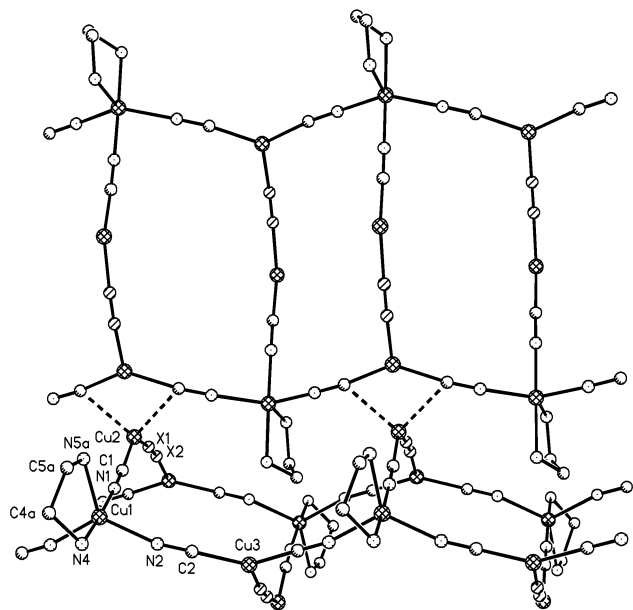


Figure 3. A perspective view of the stair-like double chain of **3** and the interconnection of the double chains to afford a 3D network. For the sake of clarity the methyl groups of the diamine ligand are omitted.

coordinated Cu(I) atom (Cu2) considerably deviates from linearity ($133.3(3)^\circ$) due to weak interactions of $2.436(4)$ Å between Cu2 and two equivalent C2 atoms of a neighboring chain, which leads to a Cu(2)⋯Cu(3) distance of $2.5021(11)$ Å between neighboring double chains and then to a 3D structure. In the trigonal-bipyramidal Cu(II) centers, the nitrogen atom N4 of the diamine ligand and the nitrogen atom N1 of a bridging cyanide group occupy axial positions whereas the remaining nitrogen atoms are bonded in equatorial positions. The single infinite chains of the double chains, running in the direction of the *b*-axis, are formed of alternating trigonal copper(I) and trigonal-bipyramidal copper(II) centers with bond angles near 120° , and then the single chains as well as the double chains are not planar but forming a infinite stair in the direction of the *b*-axis. Within the double chain, the Cu1⋯Cu2 and Cu1⋯Cu3 distances are $4.9887(13)$ and $5.0803(10)$ Å, whereas the Cu2⋯Cu3 distance is $6.8598(12)$ Å.

As indicated above, copper(I) and copper(II) ions in complexes **2** and **3** exhibit very different coordination geometries and then the compounds fit into class I of the Robin and Day classification of mixed-valence compounds. However, the presence of cyanide-bridging groups (which are known to transmit very efficiently the electronic effects) between Cu(I) and Cu(II) ions might suggest class II compounds, thus leaving the question open.

The structure of compound **4**, $[\text{NEt}_4][\text{Cu}_2(\text{CN})_3]$ (see Figure 4), consists of 2D graphite-like anionic layers $[\text{Cu}_2(\text{CN})_3]_n^{n-}$ lying on mirror planes and NEt_4^+ cations intercalated between the anionic layers. These anionic layers show the AABB pattern with interlamellar spacing of 6.129 Å. The layer structure of **4** is built from distorted trigonal Cu(I) centers linked into 18-member $\text{Cu}_6(\text{CN})_6$ rings, which fuse into a distorted 2D honeycomb structure. Each nitrogen atom of NEt_4^+ occupies symmetry element 222 midway between centers of two superimposed 18-membered rings

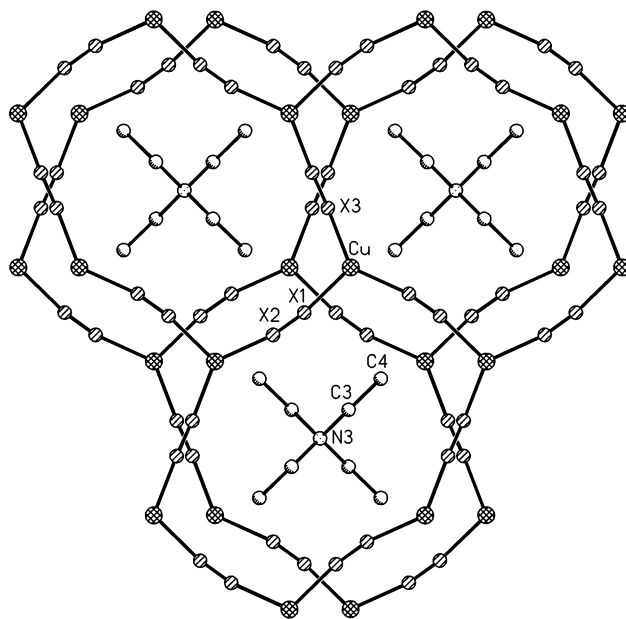


Figure 4. Anionic layers of **4** intercalated by NEt_4^+ cations.

of neighboring $[\text{Cu}_2(\text{CN})_3]_n^{n-}$ layers. The crystallographically planar 18-membered rings of **4** are different than those observed for analogous 2D layer compounds, which either are not planar¹⁸ or exhibit a ABAB repeat pattern of the layers.¹⁹ It should be noted that a similar planar structure showing the AABB pattern has been recently reported for the compound $\text{PPh}_4[\text{Cu}_2(\text{CN})_3]$.²⁰ In this complex, however, superimposed 18-membered rings of neighboring layers are oriented in the same way, while in **4** they are rotated about 90° .

In view of the above results we can draw the following conclusion: For **2** and **3**, and due to the presence of two and four methyl groups on the nitrogen atoms of the diamine ligand, respectively, complexes $[\text{Cu}(\text{N}-\text{N})_2]^{2+}$ ($\text{N}-\text{N}$ = diamine ligand) are both too voluminous (see Table 6) as to be included in the adamantane cavities, then the diamond-like structure cannot be formed and the reaction of $[\text{Cu}(\text{N}-\text{N})_2]^{2+}$ and $[\text{Cu}(\text{CN})_n]^{m-}$ species ultimately leads to the observed complexes. Likewise, the bulky $[\text{NEt}_4]^+$ cation prevents the formation of the diamond-like structure, giving rise to the observed honeycomb-layer structure. Consequently, the control of spacial factors, such as steric constraints promoted by bulky substituents, is an important key in building a great diversity of interesting cyanide-bridged copper polymeric structures.

IR Spectroscopy. The bands corresponding to $\nu(\text{CN})$ stretching vibrations for compounds **1–4** appear in the range $2081\text{--}2145\text{ cm}^{-1}$, which is typical for bridging cyanide groups. For cyanide-bridged Cu(I) complexes, such as **1** and **4**, the $\nu(\text{CN})$ decreases as the coordination number around copper(I) atoms increases. In keeping with this, for **1**, with tetrahedral copper(I) centers, the $\nu(\text{CN})$ appears at 2081

(18) Cromer, D. T.; Larson, A. C. *Acta Crystallogr.* **1962**, *15*, 397.

(19) Chesnut, D. J.; Kusnetzow, A.; Birge, R.; Zubieta, J. *Inorg. Chem.* **1999**, *38*, 5484.

(20) Zhao, Y.; Hong, M.; Su, W.; Cao, R.; Zhou, Z.; Chan, A. S. C. *J. Chem. Soc., Dalton Trans.* **2000**, 1685.

cm^{-1} , whereas for **4**, with trigonal copper(I) centers, the $\nu(\text{CN})$ vibration appears as a relatively wide band centered at 2118 cm^{-1} . This trend has also been observed for other copper(I) complexes, such as simple $[\text{Cu}(\text{CN})_n]^{n+1}$ anions,²¹ and is more likely due to the decrease of the average Cu(I)–C/N bond distances as the coordination number decreases (for crystallographically characterized cyanocuprates, Cu(I)–C/N distances are found to range from 1.80 to 1.86 Å in nearly linear dicoordinated systems, increasing to 1.92–1.96 Å in three-coordinated complexes and further to 1.94–2.0 Å for four-coordinated cyanocuprates).²² In fact, it has been recently shown that a correlation exists between $\nu(\text{CN})$ and Ag(I)–C/N bond lengths in several Ag(I)–cyanide complexes, such that $\nu(\text{CN})$ increases with decreasing Ag–C/N bond length.²³ Complexes **1** and **4**, with average Cu(I)–C/N distances of 2.04 and 1.92 Å, respectively, follow a similar trend as the $\nu(\text{CN})$ for the former appears at lower wavenumber than the latter. Complexes **2** and **3** both exhibit two $\nu(\text{CN})$ bands at about 2145 and 2125 cm^{-1} , this latter of much more intensity, which appear as a consequence of the nonequivalence of the bridging cyanide groups with different M–C/N bond distances and Cu–CN/NC bond angles. Both complexes, containing Cu(I)–CN–Cu(II) bridges, have two similar short and one long average bond distances (sum of the Cu(I)–C and Cu(II)–N bond distances) of 1.96 and 2.045 Å, respectively, for **2** and 1.93 and 1.99 Å for **3**. In this case, however, no correlation between $\nu(\text{CN})$ and M–C/N bond distances can be established. Factors others than Cu–C/N bond distances must affect $\nu(\text{CN})$ bands.

Electronic Spectroscopy. The electronic reflectance spectrum of **1** in the visible region exhibits a broad d–d absorption band centered at $17.85 \times 10^3 \text{ cm}^{-1}$. The energy of this transition agrees well with those found for other square-planar CuN_4 complexes.²⁴ Complexes **2** and **3** are characterized by very similar electronic reflectance spectra, consisting of a strong absorption, that spread the entire visible region, with a maximum centered at 15.40×10^3 and $14.50 \times 10^3 \text{ cm}^{-1}$, respectively, and a lower energy, lower intensity shoulder at around $10 \times 10^3 \text{ cm}^{-1}$. These spectra are consistent with a square-pyramidal rather than a trigonal-bipyramidal CuN_5 stereochemistry.²⁴ The latter type generally exhibits an intense and broad band at around $11 \times 10^3 \text{ cm}^{-1}$ with, if observed, a higher energy, lower intensity shoulder at around $15 \times 10^3 \text{ cm}^{-1}$. The fact that complex **3**, with a geometry very near to regular trigonal-bipyramidal geometry, presents almost the same spectra as **2**, with a distorted square-pyramidal geometry, might be supporting evidence for an intervalence charge-transfer band through the bridging cyanide groups at around $15 \times 10^3 \text{ cm}^{-1}$ in both complexes.

Emission Spectra. It is well-known that numerous mono- and polynuclear copper(I) complexes exhibit luminescence

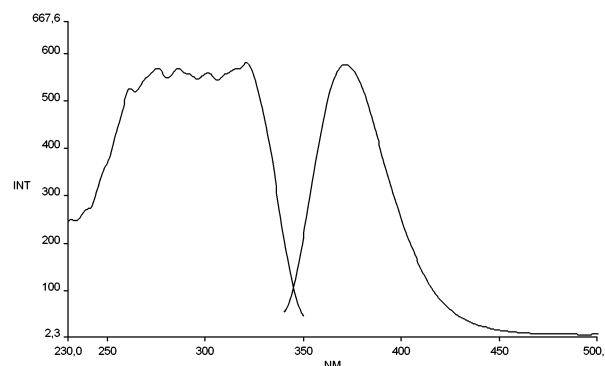


Figure 5. Excitation (with $\lambda_{\text{em}} = 372 \text{ nm}$) and emission (with $\lambda_{\text{ex}} = 320 \text{ nm}$) spectra of complex **4** in the solid state at 298 K. Intensity is in arbitrary units.

in the solid state and in solution.²⁵ Metal-to-ligand charge transfer is the most common assignment of the lowest electronic excited state, but copper-centered emission ($d^{10} \rightarrow d^9s^1$), ligand-centered emission, and interligand charge transfer are possible.²⁶ We have studied the luminescence properties of compounds **1–4**. Mixed-valence complexes, **2** and **3**, show no luminescence whereas complex **1** exhibits very weak luminescence at 77 K. The emission spectrum for **1** has a maximum at 521 nm with excitation maximum at 332 nm. The room temperature emission spectrum of **4** (see Figure 5), however, exhibits an intense maximum at 371 nm with a full width at half-maximum of 45 nm. The 77 K luminescence is more intense (as expected because of the decrease of the nonradiative thermal activated process), with its band maximum at 380 nm, an energy close to that observed at room temperature. The emission in **1** and **4** can be tentatively assigned to copper-to-cyanide transfer because the oxidation state of the copper atoms bridged by cyanide in both compounds is +1. Nevertheless, intraligand transitions cannot be ruled out. The maximum at 527 nm for **1** appears, however, at relatively low energy as to be assigned to intraligand transitions. Finally, transitions involving interactions between coppers can probably be eliminated because of the relatively long distance between metal atoms in **1** and **4**.

Magnetic Properties. The magnetic behavior of **1** is consistent with that expected for a noninteracting d^9 ion, as the room temperature effective magnetic moment remains constant and equal to $1.76 \mu_B$ from room temperature to 2 K.

The temperature dependence of the magnetic susceptibilities for **2** and **3** is given in Figures 6 and 7, respectively, in the form of a $\chi_M T$ vs T plot, χ_M being the corrected magnetic susceptibility per Cu(II) atom. In both cases, the $\chi_M T$ values at room temperature are $0.41 \text{ cm}^3 \text{ mol}^{-1} \text{ K}$ and remain almost constant until 50 K, then they continuously decrease to 0.35 (**2**) and $0.098 \text{ cm}^3 \text{ mol}^{-1} \text{ K}$ (**3**) at 1.7 K. For compound **3**, the χ_M curve presents a maximum at 2.5 K (see the inset of

(21) Nakamoto K. *Infrared and Raman Spectra of Inorganic and Coordination Compounds*, 4th ed.; John Wiley and Sons: New York, 1986; p 273.

(22) Kroeker, S.; Wasylishen, R. E.; Hanna, J. V. *J. Am. Chem. Soc.* **1999**, *121*, 1582.

(23) Bowmaker, G. A.; Effendy; Reid, J. C.; Rickard, C. E. F.; Skelton, B. W.; White, A. H. *J. Chem. Soc., Dalton Trans.* **1998**, 2139.

(24) Hathaway, B. J. In *Comprehensive Coordination Chemistry*; Wilkinson, G., Ed.; Pergamon Press: Oxford, 1987; Vol. 5.

(25) Vitale, M.; Ford, P. C. *Coord. Chem. Rev.* **2001**, *219*, 3. Ford, P. C.; Cariati, E.; Bourassa, J. *Chem. Rev.* **1999**, *99*, 3625. McMillin, D. R.; Kirchoff, J. R.; Goodwin, K. V. *Coord. Chem. Rev.* **1985**, *64*, 83.

(26) Henary, M.; Wootton, J. L.; Khan, S. I.; Zink, J. I. *Inorg. Chem.* **1997**, *36*, 796.

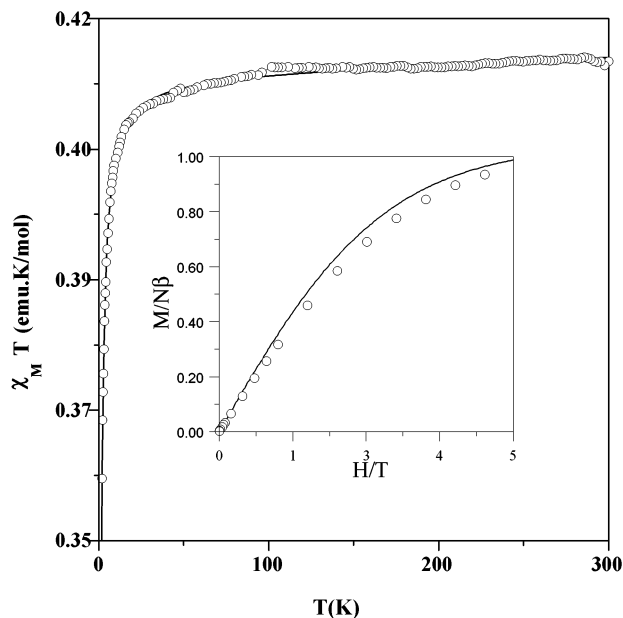


Figure 6. Temperature dependence of $\chi_M T$ and field dependence of M (inset) for **2**. Solid lines represent the theory (see text).

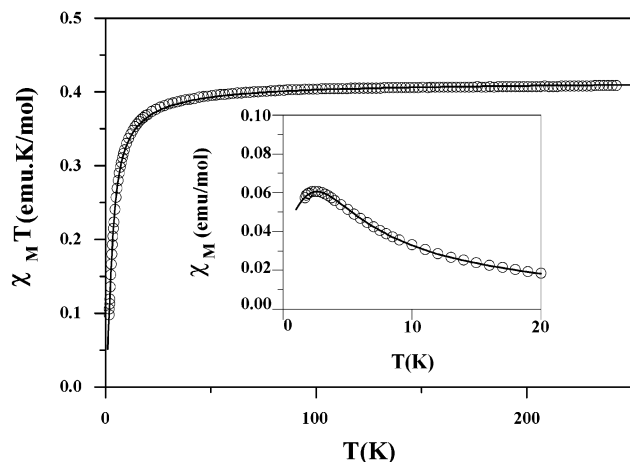


Figure 7. Temperature dependence of $\chi_M T$ and χ_M (inset) for **3**. Solid lines represent the theory (see text).

Figure 7), while no susceptibility maximum was observed for **2**. These features indicate that weak antiferromagnetic exchange interactions between copper(II) ions mediated by CN–Cu(I)–CN diamagnetic bridges occur. Taking into account the triangular arrangements of Cu(II) ions within each corrugated sheet of **2**, we have used an isotropic triangular planar model with local spin $S = 1/2$, based on high-temperature series expansions using the Hamiltonian $\mathbf{H} = -J\sum_{i,j}\mathbf{S}_i\mathbf{S}_j$.²⁷ The values obtained by fit are $J = -0.065$ (3) cm^{-1} and $g = 2.105(2)$ with $R = 1.0 \times 10^{-6}$ (R is the agreement factor defined as $\sum_i[(\chi_M T)^{\text{exp}}(i) - (\chi_M T)^{\text{calc}}(i)]^2 / \sum_i[(\chi_M T)^{\text{exp}}(i)]^2$). In keeping with the observed weak antiferromagnetic interaction, the magnetization curve as a function of the applied field at 2 K (see the inset of Figure 6) lies slightly below that of the Brillouin function for a spin doublet.

(27) (a) Rushbrooke, G. S.; Baker, G. A.; Wood, P. J. In *Phase Transitions and Critical Phenomena*; Domb, C., Green, M. S., Eds.; Academic Press: New York, 1974; Vol. III, Chapter 5. (b) Yamaji, K.; Kondo, J. *J. Phys. Soc. Jpn.* **1973**, *35*, 25.

From a magnetic point of view, **3** can be described, to a first approximation, as a Cu(II) regular chain where the paramagnetic Cu(II) ions are linked by the diamagnetic N–C–Cu(I)–C–N bridge. The fitting of the experimental data through an antiferromagnetic $S = 1/2$ uniform chain model (the Hamiltonian being $\mathbf{H} = -J\sum_i\mathbf{S}_i\mathbf{S}_{i+1}$)²⁸ with a molecular field correction to incorporate interchain exchange interactions leads to $J = -2.739(5) \text{ cm}^{-1}$, $g = 2.117(2)$, $zJ' = -0.31(2) \text{ cm}^{-1}$, and $R = 3.1 \times 10^{-5}$.

As far as we know, quite a few examples of bimetallic systems containing diamagnetic cyanometalate bridging units between paramagnetic ions with only e_g -type magnetic orbitals have been reported so far. For compounds $\text{PPh}_4[\text{Ni}(\text{pn})_2][\text{Co}(\text{CN})_6]\cdot\text{H}_2\text{O}$,²⁹ $[\text{Ni}(\text{en})_2]_3[\text{Co}(\text{CN})_6]_2\cdot 2\text{H}_2\text{O}$,³⁰ and $[\{\text{Cu}(\text{dien})_2\text{Co}(\text{CN})_6\}_n][\text{Cu}(\text{dien})(\text{H}_2\text{O})\text{Co}(\text{CN})_6]_n\cdot 5\text{H}_2\text{O}$ ³¹ with a 1D zigzag chain, rope-ladder chain, and one corner-sharing square unit chain structures, respectively, weak antiferromagnetic exchange interactions were reported. These interactions are more likely due to a combination of intra- and interchain interactions; the latter, antiferromagnetic in nature, is mainly mediated by hydrogen bonds involving water, nonbridging cyanide, and amino groups of the respective diamines. However, for compounds $[\text{Ni}(\text{en})_2]_3[\text{Fe}(\text{CN})_6](\text{PF}_6)_2$ ³² and $[\text{Cu}(\text{en})(\text{H}_2\text{O})]_2[\text{Fe}(\text{CN})_6]\cdot 4\text{H}_2\text{O}$,³³ with $[\text{Fe}(\text{CN})_6]^{4-}$ bridging units and 3D and 1D structures, respectively, as well as for $(\text{tmen})\text{Cu}[\text{Au}(\text{CN})_2]_2$,³⁴ with $[\text{Au}(\text{CN})_2]^-$ bridging groups and 1D structure, weak ferromagnetic interactions were observed between paramagnetic ions. In the two former cases, the σ -exchange pathway between the nearest paramagnetic M(II) ions (M(II) = Ni(II) or Cu(II)) takes place through the empty $d\sigma$ orbital of the Fe(II) (t_{2g}^6) and this, according to Goodenough–Kanamori’s rules, leads to a ferromagnetic interaction. This interpretation, however, can be applied neither to $(\text{tmen})\text{Cu}[\text{Au}(\text{CN})_2]_2$, where the Au(I) center exhibits a d^{10} configuration, nor to the above-mentioned $[\text{Co}(\text{CN})_6]^{3-}$ -containing systems (Co^{III} also in a t_{2g}^6 configuration) exhibiting antiferromagnetic exchange interactions. Note that it has been recently shown that in a heptanuclear Fe(II)Fe(III)₆ mixed-valence system,³⁵ the diamagnetic hexacyanoferrate(II) unit mediates ferromagnetic interactions between the Fe(III) centers. This behavior was justified by the interaction of the ground configuration with the excited configuration, generated by electron transfer from the low-spin Fe^{II} ion to one of the high-spin Fe^{III} ions. For the Cu(I)–Cu(II) mixed-valence compounds reported here, where no hydrogen

(28) Bonner, J.; Fisher, M. E. *Phys. Rev.* **1964**, *135*, A640.

(29) Ohba, M.; Usuki, N.; Fukita, N.; Okawa, H. *Inorg. Chem.* **1998**, *37*, 3349.

(30) Ohba, M.; Fukita, N.; Okawa, H. *J. Chem. Soc., Dalton* **1997**, 1733.

(31) Ferbinteanu, M.; Tanase, S.; Andruh, M.; Journaux, Y.; Cimpoesu, F.; Strenger, I.; Rivière, E. *Polyhedron* **1999**, 3019.

(32) Fukita, N.; Ohba, M.; Okawa, H.; Matsuda, K.; Iwamura, H. *Inorg. Chem.* **1998**, *37*, 842.

(33) Luo, J.; Hong, M.; Chen, C.; Wu, M.; Gao, D. *Inorg. Chim. Acta* **2002**, *328*, 185.

(34) Leznoff, D. B.; Xue, B.-Y.; Patrick, B. O.; Sanchez, V.; Thompson, R. C. *J. Chem. Soc., Chem. Commun.* **2001**, 259.

(35) Røge, G.; Marvilliers, A.; Riviere, E.; Audière, J. P.; Lloret, F.; Varret, F.; Goujon, A.; Mendenez, N.; Girerd, J. J.; Mallah, T. *Angew. Chem., Int. Ed.* **2000**, *39*, 2885.

bonding interactions exist, the observed magnetic exchange interaction might be the result of the sum of two contributions: one arising from the pure ground-state configuration, which, in view of the previous results, would be either weak ferro- or antiferromagnetic, and the other one from the charge-transfer configuration $\text{Cu}^{\text{I}}-\text{CN}-\text{Cu}^{\text{II}}-\text{CN}-\text{Cu}^{\text{II}}$ that mixes with the ground-state configuration. This latter contribution, antiferromagnetic in nature, would be of greater magnitude than the former, thus leading to an overall antiferromagnetic exchange interaction.

Finally, the difference in magnitude of the antiferromagnetic interaction observed for **2** and **3** can be tentatively justified by taking into consideration the nature of the magnetic orbitals and the geometrical features of the $\text{Cu}(\text{I})-\text{CN}-\text{Cu}(\text{II})$ bridging fragment. For **2**, with copper(II) atoms exhibiting a distorted square-pyramidal geometry, the spin density of the unpaired electron is mainly located at the $d_{x^2-y^2}$ orbital directed toward the nitrogen atoms of the CN bridging groups in the basal plane. For **3**, the copper(II) ion, however, displays a trigonal bipyramid geometry with a d_{z^2} magnetic orbital directed to the axial positions. Thus, while in compound **2** the majority of the exchange pathways involve basal positions, in **3** the exchange pathways involve equatorial positions where the spin density is half of that in apical positions. In view of the above consider-

ations, in principle, the magnetic exchange interaction for **2** should be larger than that for **3**. However, a closer examination of the structures clearly reveals that $\text{Cu}^{\text{I}}-\text{CN}$ and $\text{Cu}^{\text{II}}-\text{CN}$ bond angles for the former are more deviated from linearity than those for the latter. This would reduce the magnetic exchange interaction in **2** to such an extent that the antiferromagnetic interaction for **3** would be superior.

Nevertheless, more examples of bimetallic and mixed-valence complexes with diamagnetic cyanometalate bridging units are needed to clarify the nature of the weak magnetic interactions mediated by these types of bridges.

Acknowledgment. This study was financially supported by the Dirección General de Investigación Científica y Técnica (Spanish Government, project PB97/0822), Junta de Andalucía, and the Academy of Finland (project 41519, R.K.). We gratefully acknowledge R. Uggla for his help with DFT calculations.

Supporting Information Available: X-ray crystallographic files, in CIF format, for compounds $[\text{Cu}(\text{pn})_2][\text{Cu}_2(\text{CN})_4]$ (**1**), $[\text{Cu}_2(\text{CN})_3(\text{dmen})]$ (**2**), $[\text{Cu}_3(\text{CN})_4(\text{tmen})]$ (**3**), and $[\text{NEt}_4][\text{Cu}_2(\text{CN})_3]$ (**4**). This material is available free of charge via the Internet at <http://pubs.acs.org>.

IC025743V